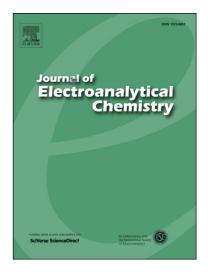# Accepted Manuscript

Temozolomide chemical degradation to 5-aminoimidazole-4-carboxamide – Electrochemical study

Ilanna C. Lopes, Severino Carlos B. de Oliveira, Ana Maria Oliveira-Brett

Temozolomide chemical degradation to

5-aminoimidazole-4-carboxamide

– Electrochemical study

Ilanna C. Lopes, Severino Carlos B. de Oliveira, Ana Maria Oliveira-Brett[*]

Departamento de Química, Faculdade de Ciências e Tecnologia,

Universidade de Coimbra, 3004-535 Coimbra, Portugal

* brett@ci.uc.pt

Ana Maria Oliveira-Brett

Departamento de Química, Faculdade de Ciências e Tecnologia

Universidade de Coimbra

3004-535 Coimbra

Portugal

Tel/FAX: + 351-239-835295

Abstract

The evaluation of the chemical degradation of temozolomide (TMZ), a potential anti-cancer drug, to its major metabolite 5-aminoimidazole-4-carboxamide (AIC), in aqueous solution with different pH values, was investigated at a glassy carbon electrode using cyclic and differential pulse voltammetry, and UV-Vis spectrophotometry. TMZ was incubated in aqueous solution, for different periods of time, and the changes in TMZ electrochemistry behaviour detected. The TMZ reduction is a pH-dependent irreversible process on the tetrazinone ring causing its irreversible breakdown. TMZ oxidation is a pH-dependent irreversible process that occurs in two consecutive charge transfer reactions. TMZ chemical degradation was electrochemically detected by the increase of the TMZ anodic peak current and the disappearance of the TMZ cathodic peak. The rate of chemical degradation increases with increasing pH and the mechanism corresponds to TMZ chemical degradation to AIC. The electrochemical behaviour of AIC over a wide pH range, was also investigated using cyclic, differential pulse and square wave voltammetry, AIC oxidation is an irreversible, diffusion-controlled process, pH-dependent up to a pH close to the pK_a, and occurs in two consecutive charge transfer reactions, with the formation of two reversible redox products. A mechanism for AIC oxidation is proposed.

1. Introduction

DNA alkylating agents have historically played an important role in systemic chemotherapy for cancer [1]. The methylating agent temozolomide (TMZ), Scheme 1, is a member of a series of synthetic imidazotetrazinone derivatives which have a broad-spectrum antitumour activity in preclinical screening [2]. TMZ prolongs survival when administered during and after radiotherapy, which is used as a first-line treatment for glioblastoma [3]. The drug has also been approved for the treatment of recurrent high-grade glioma and is in phase II/III clinical trials for the treatment of melanoma and other solid neoplasias [4].

TMZ is an anticancer prodrug that is spontaneously hydrolyzed at physiological pH to the highly unstable compound 5-(3-methyltriazen-1-yl)imidazole-4-carboxamide (MTIC) [5], Scheme 1. Thereafter, MTIC rapidly degrades to 5-aminoimidazole-4-carboxamide (AIC) and methyldiazonium ion [6, 7] which is an active alkylating species [5]. This species produces methyl adducts at the accessible nucleophilic atoms in DNA. Thus, the antitumour activity of TMZ is largely attributed to the methylation of DNA which, as described previously, is dependent upon formation of a reactive methyldiazonium cation [6, 8]. The electrochemical study of TMZ interaction with DNA was undertaken and a mechanism of TMZ-DNA interaction was proposed [9].

Here Scheme 1

The decomposition of TMZ is irreversible and caused mainly by its pH-dependent hydrolysis to MTIC and hepatic metabolism only plays a minor role. TMZ is stable under acidic conditions but rapidly decomposes under neutral and basic conditions [10].

TMZ is rapidly and completely absorbed from the gastrointestinal tract after oral administration and the time necessary to reach peak plasma concentration (t_{max}) is 1 h. It is rapidly eliminated with a half-life ($t_{1/2} = \ln 2/k$, where k is the elimination rate constant) of 1.7-1.9 h and exhibits linear kinetics over the therapeutic dosing range [11, 12]. A TMZ half-life of only 15 min in *in vitro* serum [13] and 33 min and 28 min in water at pH = 7.9 [14] was reported. MTIC half-lives of 1.9 h in human plasma *in vivo* [15, 16], 25 min in human plasma *in vitro* [13, 15], and 13 min in water pH = 7.9 [14] were determined. AIC is stable in human plasma [15] and in water at pH = 7.9 [14], at room temperature.

Considering that TMZ is a prodrug and that its degradation products in aqueous solution are responsible for its pharmacological activity, a few methods have been described for the analysis of TMZ and its metabolites in aqueous media, such as micellar electrokinetic capillary electrophoresis (MEKC) [14, 16] and reverse-phase high performance liquid chromatography (HPLC) with UV [13, 15, 17] or MS/MS detection [18], was reported. However, an electrochemical investigation of the of TMZ chemical degradation processes in aqueous medium has not been carried out.

Due to their high sensitivity, voltammetric methods have been successfully used for the detection and determination of various pharmaceutical and biological compounds and their metabolites. Moreover, the investigation of the redox behaviour of biologically relevant compounds by means of electrochemical techniques has the

potential for providing valuable insights into the redox reactions of these molecules [19-23].

In the present paper a systematic electrochemical study of the kinetics of TMZ chemical degradation processes and of the electrochemical behaviour of AIC, the TMZ major metabolite/degradation product has been undertaken, in aqueous solution at different pH, using cyclic voltammetry, differential pulse and square wave voltammetry at a glassy carbon electrode.

2. Experimental

2.1. Materials, reagents and solutions

All reagents were of high purity grade, TMZ ($\geq$ 98%) was purchased from Sigma-Aldrich, while all the other reagents were obtained from Merck.

A stock solution of 1 mM TMZ was prepared in deionised water and kept at 4°C until further use. A stock solution of 1 mM chemically degraded TMZ (cdTMZ) was obtained after incubation of 1 mM TMZ in 0.1 M phosphate buffer pH = 7.0 for 7 days, at room temperature.

Supporting electrolyte solutions of different pH / composition (3.0 / HAcO + NaAcO, 4.1 / HAcO + NaAcO, 5.3 / HAcO + NaAcO, 6.0 / NaH_2PO_4 + Na_2HPO_4, 7.0 / NaH_2PO_4 + Na_2HPO_4, 8.0 / NaH_2PO_4 + Na_2HPO_4, 9.2 / NaOH + $Na_2B_2O_7$, 10.1 / NaOH + $Na_2B_2O_7$) were prepared using purified water from a Millipore Milli-Q system (conductivity $\leq$ 0.1 μS cm^{-1}) with ionic strength I = 0.1 M.

The pH measurements were performed with a Crison micropH 2001 pH-meter (Barcelona, Spain) with an Ingold combined glass electrode. Microvolumes were

measured using P20, P200 and P1000 Microliter Pippettes (Gilson S.A., Villiers-le-Bel, França).

All experiments were carried out at room temperature ($25 \pm 1°C$).

2.2. Voltammetric measurements

The electrochemical experiments were done using an IVIUM CompactStat potentiostat in combination with IviumSoft program version 1.84 (Ivium Technologies, Eindhoven, The Netherlands). Voltammograms were recorded using a three-electrode system (Cypress System, Inc., USA). The working electrode was a glassy carbon electrode (GCE, d = 1.5 mm diameter); Ag/AgCl (3M KCl) was used as a reference electrode and a Pt wire as a counter electrode. The electrodes were used in a one-compartment electrochemical cell of 2 mL capacity.

Cyclic voltammetry (CV) was carried out at scan rate 100 mV s^{-1}. Differential pulse (DP) voltammetry, was done using pulse amplitude 50 mV, pulse width 80 ms and scan rate 5 mV s^{-1}; whilst square wave (SW) voltammetry used frequency 50 Hz and potential increment of 2 mV, corresponding to an effective scan rate of 100 mV s^{-1}.

The GCE was polished using diamond spray (particle size 3 μm, Kemet International Ltd, UK) before each electrochemical experiment. After polishing, it was rinsed thoroughly with Milli-Q water. Following this mechanical treatment, various voltammograms were recorded in supporting electrolyte solution, in order to obtain a stable baseline voltammogram. This procedure ensured very reproducible experimental results.

2.3. Acquisition and presentation of voltammetric data

The DP voltammograms presented were baseline-corrected using the moving average application included in Ivium version 1.84 software. This mathematical

treatment improves the visualization and identification of peaks over the baseline without introducing any artefact, although the peak intensity is in some cases reduced (< 10 %) relative to that of the untreated curve. Nevertheless, this mathematical treatment of the original voltammograms was used in the presentation of all experimental voltammograms for a better and clearer identification of the peaks. The values for peak current presented in all graphs were determined from the original untreated voltammograms after subtraction of the baseline.

2.4. UV-Vis spectrophotometry

UV-Vis measurements were performed using a Spectrophotometer SPECORD S100 running with Aspect Plus Version 1.5 (Analytik Jena GmbH, Jena, Germany). The experimental conditions for absorption spectra were: integration time 41 ms and accumulation 10 points. All UV-Vis spectra were measured in a quartz glass cuvette with an optical path of 1 mm.

3. Results and discussion

3.1. TMZ chemical degradation

3.1.1. Electrochemical study

The evaluation of TMZ chemical degradation in aqueous solution was first studied by CV, in 600 µM TMZ incubated in 0.1 M acetate buffer pH = 4.1, 0.1 M phosphate buffer pH = 7.0, and 0.1 M borax buffer pH = 9.2, for different periods of time and the changes in TMZ electrochemistry behaviour were monitored.

The oxidation behaviour of TMZ in a freshly prepared solution of TMZ was investigated in 0.1 M phosphate buffer pH = 7.0, saturated with N_2, as a necessary control to enable identification of the peaks after TMZ chemical degradation.

CVs were recorded at an initial potential of 0.00 V, scanning in the positive direction until + 1.00 V, then reversing the scan direction to the negative potential limit of - 1.25 V, at a scan rate v = 100 mV s^{-1}, and three peaks were observed, Fig. 1A. The redox behaviour of TMZ occurs in a multi-step mechanism where peak 1a, at E_{p1a} = + 0.45 V, correspond to the oxidation of the tetrazinone ring causing its irreversible breakdown [19]. Peak 2a, at E_{p2a} = + 0.80 V, is attributed to the irreversible oxidation of the nitrogen in the already opened tetrazinone ring [19], and peak 3c, at E_{p3c} = - 0.76 V, correspond to the reduction in the tetrazinone ring, [19]. The second CV recorded in the same solution, without cleaning the GCE surface, showed a decrease of the peak 1a, 2a and 3a currents, due to adsorption of TMZ oxidation/reduction products on the GCE surface. However, no new peak was detected, so no electroactive products were formed in the TMZ redox processes [19].

The CV in the same TMZ solution after 7 days incubation in 0.1 M phosphate buffer pH = 7.0 0, Fig. 1A, showed two consecutive irreversible anodic peaks with very large currents, peak 1a, at E_{p1a} = + 0.54 V, and peak 2a, at E_{p2a} = + 0.91 V. On the first reverse negative-going cycle a new cathodic peak 4c, at E_{p4c} = - 0.04 V, appeared, and the cathodic peak 3c was not detected. These results suggested that chemical degradation of TMZ occurs at physiological pH since the electrochemical behaviour of TMZ changed significantly after a long incubation period in 0.1 M phosphate buffer pH = 7.0.

A CV in a freshly-prepared TMZ solution in 0.1 M acetate buffer pH = 4.1, saturated with N_2, showed the cathodic peak 3c, at E_{p3c} = - 0.64 V [19], Fig. 1B, and no

anodic peak. After 7 days incubation only one anodic peak, peak 1a, at $E_{p1a} = + 0.58$ V, was observed, indicating a lesser chemical degradation of TMZ in acidic media, since the cathodic peak 3c remained and the current was unchanged, Fig. 1B.

In 0.1 M borax buffer pH = 9.2, a CV in a freshly prepared TMZ solution, saturated with N_2, showed two anodic peaks, peak 1a, at $E_{p1a} = + 0.49$ V, and peak 2_a, at $E_{p2a} = + 0.74$ V and the cathodic peak 3_c, at $E_{p3c} = - 0.89$ V [19], Fig. 1C. After 2 h incubation an increase of the oxidation currents peak 1a, at $E_{p1a} = + 0.42$ V, and peak 2a, at $E_{p2a} = + 0.79$ V, was observed, Fig. 1C. On the first reverse negative-going cycle a new cathodic peak 4c, at $E_{p4c} = - 0.19$ V, appeared, and the cathodic peak 3c was not seen. In the second reverse positive-going cycle a new oxidation peak 4a, at $E_{p4a} = + 0.12$ V, appeared. The results are similar to pH 7.0, but a more rapid chemical degradation of TMZ occurs after 2 h incubation in alkaline media, compared to that in physiological media after 7 days TMZ incubation.

Here Figure 1

In order to study the degradation process of TMZ in physiological media, DP voltammograms were also recorded in 250 µM TMZ in 0.1 M phosphate buffer pH = 7.0 for different incubation times. DP voltammograms in a fresh TMZ solution showed only one small oxidation peak 1a, at $E_{p1a} = + 0.42$ V, Fig. 2. After 1 h incubation the CV showed two anodic peaks, peak 1a, at $E_{p1a} = + 0.37$ V, and peak 2a, at $E_{p2a} = + 0.74$ V, and after longer incubation times, 1 to 7 days, a progressive increase of the peak 1_a and 2_a currents occurred with increasing incubation time, Fig. 2, reaching constant values after 7 days incubation, meaning that the chemical degradation of TMZ was complete.

Here Figure 2

The time dependent chemical degradation of TMZ in solution is clearly demonstrated by the increase of the peak 1_a and 2_a currents and the disappearance of peak 3_a, due to the formation of AIC [24], Scheme 1.

3.1.2. Spectrophotometric study

Spectrophotometric measurements of the chemical degradation of TMZ were carried out in order to complement the voltammetric studies. UV-Vis absorption spectra were recorded at different pHs in a freshly prepared 50 μM TMZ aqueous solution and after different incubation times.

The absorption spectra of a freshly prepared solution of TMZ in 0.1 M phosphate buffer pH = 7.0 showed three absorption bands with maxima at $\lambda = 212$, 254 and 330 nm (bands 1, 2 and 3) [16], Fig. 3A. After 2 days incubation, two new absorption bands with maxima at $\lambda = 204$ nm (band 4) and $\lambda = 226$ nm (band 5) appeared and at the same time band 2 increased in height and band 3 decreased, Fig. 3A. After 7 days, the absorption spectra showed a progressive increase of the absorbance and better definition of bands 4 and 5, accompanied by a significant simultaneous increase of the absorbance of band 2, and total disappearance of band 3, Fig. 3A. These results confirmed that the TMZ chemical degradation occurs in physiological media and also indicated that the chemical degradation was completed after 7 days incubation, in agreement with the results obtained by DP voltammetry.

Here Figure 3

The absorption spectra of a freshly prepared solution of TMZ in 0.1 M acetate buffer pH = 4.1 showed three absorption bands with maxima at λ = 216, 254 and 330 nm (bands 1, 2 and 3), Fig. 3B. After 7 days incubation two new absorption bands with maxima at λ = 214 nm (band 4) and λ = 225 nm (band 5) appeared, but bands 2 and 3 only decreased slightly, Fig. 3B.

In 0.1 M borax buffer pH = 9.2 the absorption spectra of a freshly prepared solution of TMZ showed three absorption bands with maxima at λ = 210, 254 and 328 nm (bands 1, 2 and 3), Fig. 3C. After 30 min incubation, the spectra showed two new absorption bands with maxima at λ = 194 nm (band 4) and λ = 226 nm (band 5) appeared and at the same time band 2 increased in height and band 3 decreased, Fig. 3C. After 2 h, the absorption spectra showed a progressive increase of the absorbance of bands 4 and 5 and at the same time band 2 increased and band 3 disappeared completely, Fig. 3C.

3.1.3. TMZ degradation mechanism

The electrochemical and UV-Vis experiments showed that TMZ undergoes chemical degradation in aqueous solutions at different pH values and the degradation rate increases with increasing pH.

The TMZ chemical degradation in aqueous solution was verified by UV-Vis experiments since changes in the three TMZ absorption bands occurred accompanied by the appearance of two new bands.

The electrochemical experiments showed the simultaneous increase of TMZ peak 1a and 2a currents, decrease and disappearance of the cathodic peak 3c, and

appearance of the new peak 4c-4a, attributed to the reduction/oxidation of AIC, the TMZ chemical degradation product, Fig. 1.

The UV-Vis and the electrochemical results are in agreement. A rapid TMZ chemical degradation to AIC occurs in alkaline media after 2 h incubation, compared to 7 days TMZ incubation in physiological media.

AIC is formed in a TMZ hydrolysis cascade mechanism, Scheme 1. The first product is methyl triazene (MTIC), which transfers its methyl group to a nucleophile to form the final product AIC [24].

3.2. Electrochemical behaviour of TMZ chemical degradation product

The electrochemical behaviour of 250 µM TMZ chemical degradation product (cdTMZ), obtained after incubation of TMZ in 0.1 M phosphate buffer pH = 7.0 for 7 days, at room temperature, was investigated in a wide range of supporting electrolytes, using CV, DP and SW voltammetry.

3.2.1. Cyclic voltammetry

CV of cdTMZ in 0.1 M phosphate buffer pH = 7.0, starting at 0.00 V and cycling between a positive potential limit of + 1.00 V and a negative potential limit of - 0.03 V, showed in the positive-going scan of the first cycle peaks 1a and 2a, corresponding to the irreversible oxidation of cdTMZ, Fig. 4, and on the reverse negative-going scan peak 4c, for the reduction of the cdTMZ oxidation product, as shown in *Section 3.1.1*. In the second scan in the positive region a new oxidation peak 4a, at E_{p4a} = + 0.01 V, appeared corresponding to oxidation of the cdTMZ reduction product formed at the GCE surface, thus confirming the reversibility of peak 4c. On successive scans in the same solution, the decrease of the peak 1a and 2a

currents, due to the adsorption of the oxidation product AIC on the electrode surface, was observed, Fig. 4.

Here Figure 4

In order to clarify which peak, 1a or 2a, led to the oxidation product corresponding to the reversible peaks 4c-4a, CVs were recorded under the same conditions with a clean GCE surface, but the scan direction was inverted immediately after peak 1a and before peak 2a. The peaks 4c-4a appeared when the scan direction was inverted immediately after peak 1a, confirming that the electroactive oxidation product of peaks 4c-4a is associated with peak 1a.

The effect of scan rate on peak 1a potential and current was also investigated and CVs were recorded without cleaning the electrode surface between measurements. Increasing the scan rate, the peak 1a potential was slightly shifted to more positive values, in agreement with the irreversible nature of the electrochemical process.

The difference between peak 1a potential and the peak potential at half height was $|E_{p1a} - E_{p1a/2}| \approx 80$ mV. Since for a diffusion-controlled irreversible system $|E_{pa} - E_{p/2a}| = 47.7/(\alpha_a n')$ where α_a is the charge transfer coefficient and n' the number of electrons in the rate-determining step [25], it can be calculated that $\alpha_a n' = 0.60$.

Increasing the scan rate, the current of peak 1a increased linearly with the square root of scan rate, consistent with the diffusion-limited oxidation process of a solution species. The peak current in amperes for a diffusion-controlled irreversible system is given by I_{pa} (A) = + 2.99 x 10^5 $n(\alpha_a n')^{1/2}$ A $[R]_\infty$ $D_R^{1/2}$ $v^{1/2}$ where n is the number of electrons transferred during the oxidation of cdTMZ ($n = 2$ as shown in *Section 3.2.2*), A is the electrode area in cm^2, D_R is the diffusion coefficient of R in cm^2 s^{-1}, $[R]_\infty$ is the

concentration in mol cm^{-3} and v is in V s^{-1} [25]. By plotting I_{pa} *vs.* $v^{1/2}$, the value of D_R is

obtained. For this calculation, the GCE electroactive area was determined from a plot of

I_{pa} *vs.* $v^{1/2}$ using a solution of 500 µM hexacyanoferrate (II) and the value of the

diffusion coefficient of hexacyanoferrate (II) in pH = 7.0 0.1 M phosphate buffer of

7.35 x 10^{-6} cm^2 s^{-1} [26], and the GCE electroactive area of 1.26 x 10^{-2} cm^2 was

determined. From the measured slope of 5.96 x 10^{-6} A/(V s^{-1})$^{1/2}$,

the diffusion coefficient of cdTMZ in 0.1 M phosphate buffer pH = 7.0 was

D_{cdTMZ} = 1.7 x 10^{-5} cm^2 s^{-1}.

Considering that the reaction corresponding to peaks 4c-4a is a reversible

process, the number of electrons involved in the redox mechanism was determined. For

a reversible system, the difference between peak potential and the potential at half

height of peak, $|E_p - E_{p/2}|$ = 56.6/n where n is the number of electrons in the rate-

determining step [25]. Since $|E_{p4a} - E_{p4a/2}| \approx 36$ mV for the peak 4a, it can be calculated

that n = 1.6. Consequently, it can be confirmed that the reversible redox reaction at peak

4a occurs with the transfer of two electrons.

The reduction of cdTMZ was also investigated by CV in 0.1 M phosphate buffer

pH = 7.0, starting potential 0.00 V and cycling between a negative potential limit of

- 1.00 V and a positive potential limit of 0.00 V, and as expected, no cathodic peak was

observed.

3.2.2. Differential pulse voltammetry

The effect of pH on the electrochemical oxidation of cdTMZ was studied over a

wide pH range between 3.0 and 10.1 using DP voltammetry, Fig. 5A.

For all pH's, peaks 1a and 2a appeared and their oxidation potentials were

shifted to more negative values with increasing pH, Fig. 4A. The slope of the dotted line

of - 59 mV per pH unit for these peaks, Fig. 5B, shows that the mechanism of each

oxidation process involves the same number of electrons and protons [27], and considering the width at half-height of each peak, both electrode reactions involve one electron and one proton.

Here Figure 5

The variation of peaks 1_a and 2_a current versus pH shows that the most sensitive response was observed in acidic media.

Successive DP voltammograms were recorded in all pH buffer electrolytes.

On the first scan, in pH = 7.0 0.1 M phosphate buffer, only peaks 1a, at $E_{p1a} = + 0.41$ V, and 2a, at $E_{p2a} = + 0.79$ V, occurred, Fig. 6. On the second scan, a new peak 5a, at $E_{p5a} = + 0.18$ V, was observed. This peak corresponds to the oxidation of the cdTMZ oxidation product formed on the GCE surface during the first potential scan. After successive scans, peaks 1a and 2a potential remained almost same. Also the peak 1a current decreased gradually and peak 2a current decreased significantly. The peak 5a current increased with the number scans, due to the formation of more oxidation products adsorbed on the GCE surface.

The adsorption of cdTMZ oxidation product on the GCE surface was confirmed when, after several DP scans recorded in the cdTMZ solution, the electrode was washed with a jet of deionized water and then transferred to the supporting electrolyte, the DP voltammogram showed peak 5a.

In order to clarify which peak, 1a or 2a, led to the oxidation product corresponding to peak 5a, DP voltamogramms were recorded under the same conditions with a clean GCE surface, but the second scan was recorded immediately after peak 1a

and before peak 2a. Peak 5a did not occurred under these conditions, Fig. 6, confirming that it is not due to the oxidation of the cdTMZ oxidation product formed at peak 1a.

Here Figure 6

The pH-dependence of peak 5_a was studied in different buffer electrolytes. For $3.0 < pH < 10.1$, the pH-dependence of peak 5_a was linear with a slope of - 59 mV per pH unit, which shows that the oxidation mechanism involves the same number of electrons and protons [27], and considering the width at half-height of each peak, the electrode reaction involves two electrons and two protons.

3.2.3. Square wave voltammetry

The advantages of SW voltammetry are greater speed of analysis, lower consumption of the electroactive species in relation to DP voltammetry, and reduced problems regarding the blocking of the electrode surface [25]. Furthermore, it permits to see during only one scan if the electron transfer reaction is reversible or not. Since the current is sampled in both positive and negative-going pulses, and the peaks corresponding to the oxidation and reduction of the electroactive species at the electrode surface can be obtained in the same experiment.

The electrochemical oxidation behaviour of cdTMZ was also investigated by SW voltammetry in different supporting electrolyte pHs.

The SW voltammogram in 250 µM cdTMZ in 0.1 M phosphate buffer pH = 7.0 showed on first scan peak 1a, at $E_{p1a} = + 0.42$ V, and peak 2a, at $E_{p2a} = + 0.82$ V, Fig. 7A. The irreversibility of both redox reactions was confirmed by plotting the forward and backward components of the total current. Whereas the

forward component showed both oxidation peaks at the same potential and with the same current as the total current obtained, on the backward component no cathodic peak occurred.

Here Figure 7

On the second consecutive SW voltammogram the oxidation peak 5a, at $E_{p5a} = + 0.21$ V, appeared, Fig. 7B. The reversibility of this reaction was also confirmed by plotting the forward and backward components of the total current, and the oxidation and the reduction currents were equal. Moreover, the identical peaks 5a-5c potentials, on the forward and backward current components, confirmed the adsorption of cdTMZ oxidation product on the GCE surface.

3.2.4. Redox mechanism of TMZ chemical degradation product

The TMZ chemical degradation investigation by CV and DP voltammetry was crucial to understand the stability of TMZ.

Considering the mechanism of TMZ chemical degradation to AIC in aqueous solution [24], Scheme 1, and AIC oxidation at the carbon surface [28], it is evident that the electrochemical behaviour of cdTMZ is associated with the AIC molecule. However, the cdTMZ reversible oxidation products, peak 4a-4c and peak 5a-5c, Figs. 4, 6 and 7, were identified for the first time, and correspond to the oxidation of AIC.

A mechanism for the oxidation of AIC is proposed. In the first step, peak 1a, one electron is removed from the amine group in the C5 position, Scheme 1. This is followed by deprotonation, leading to a product that

is reversibly reduced, peak 4a-4c, in a two electron-two proton transfer on the GCE surface.

In the second step, peak 2a, one electron is removed from the imidazole ring in the C5 position, Scheme 1. This is followed by deprotonation and direct nucleophilic attack by water, giving a product with one carbonyl group in the C5 position in the imidazole ring, which is also reversibly reduced, peak 5a-5c, in a two electron-two proton transfer on the GCE surface.

4. Conclusions

The chemical degradation of TMZ in aqueous solution at different pHs was investigated using voltammetry and complemented by UV-Vis spectrophotometry. The TMZ chemical degradation was electrochemically detected by the changes with time in the TMZ electrochemical behaviour, and the results showed that the rate of TMZ degradation increases progressively with increasing pH. An electroanalytical method to investigate TMZ pharmacokinetics was developed.

The investigation of cdTMZ electrochemical behaviour confirmed that the electroactive product formed was AIC, which undergoes oxidation in a diffusion-controlled irreversible and pH-independent process, in two consecutive charge transfer reactions, with the formation of two redox products, which are reversibly reduced. A mechanism for oxidation of AIC was proposed.

References

[1] B.D. Diez, P. Statkevich, Y. Zhu, M.A. Abutarif, F. Xuan, B. Kantesaria, D. Cutler, M. Cantillon, M. Schwarz, M.G. Pallotta, F.H. Ottaviano, Evaluation of the exposure equivalence of oral versus intravenous temozolomide, Cancer Chemother. Pharmacol. 65 (2010) 727-734.

[2] M.F.G. Stevens, J.A. Hickman, S.P. Langdon, D. Chubb, L. Vickers, R. Stone, G. Baig, C. Goddard, N.W. Gibson, J.A. Slack, C. Newton, E. Lunt, C. Fizames, F. Lavelle, Antitumor activity and pharmacokinetics in mice of 8-carbamoyl-3-methyl-imidazo[5,1-d]-1,2,3,5-tetrazin-4(3H)-one (CCRG 81045; M & B 39831), a novel drug with potential as an alternative to dacarbazine, Cancer Res. 47 (1987) 5846-5852.

[3] R. Stupp, W.P. Mason, M.J. van den Bent, M. Weller, B. Fisher, M.J. Taphoorn, K. Belanger, A.A. Brandes, C. Marosi, U. Bogdahn, J. Curschmann, R.C. Janzer, S.K. Ludwin, T. Gorlia, A. Allgeier, D. Lacombe, J.G. Cairncross, E. Eisenhauer, R.O. Mirimanoff, Radiotherapy plus concomitant and adjuvant temozolomide for glioblastoma, N. Engl. J. Med. 352 (2005) 987-996.

[4] P. Caporaso, M. Turriziani, A. Venditti, F. Marchesi, F. Buccisano, M.C. Tirindelli, E. Alvino, A. Garbin, G. Tortorelli, L. Toppo, E. Bonmassar, S.D'Atri, S. Amadori, Novel role of triazenes in haematological malignancies: pilot study of temozolomide, Lomeguatrib and IL-2 in the chemo-immunotherapy of acute leukaemia, DNA Repair 6 (2007) 1179-1186.

[5] M.J.M. Darkes, G.L. Plosker, B. Jarvis, Temozolomide: a review of its use in the treatment of malignant gliomas, malignant melanoma and other advanced cancers, Am. J. Cancer 1 (2002) 55-80.

[6] B.J. Denny, R.T. Wheelhouse, M.F. Stevens, L.L. Tsang, J.A. Slack, NMR and molecular modeling investigation of the mechanism of activation of the antitumor drug temozolomide and its interaction with DNA, Biochemistry 33 (1994) 9045-9051.

[7] H.S. Friedman, T. Kerby, H. Calvert, Temozolomide and treatment of malignant glioma, Clin. Cancer Res. 6 (2000) 2585-2597.

[8] A.S. Clark, M.F.G. Stevens, C.E. Sansom, C.H. Schwalbe, Anti-tumour imidazotetrazines. Part XXI. Mitozolomide and temozolomide: probes for the major groove of DNA, Anti-Cancer Drug Design 5 (1990) 63-68.

[9] I.C. Lopes, S.C.B. Oliveira, A.M. Oliveira-Brett, In situ electrochemical evaluation of anticancer drug temozolomide and its metabolites–DNA interaction, Anal. Bioanal. Chem. 405 (2013) 3783-3790.

[10] S.D. Baker, M. Wirth, P. Statkevich, P. Reidenberg, K. Alton, S.E. Sartorius, M. Dugan, D. Cutler, V. Batra, L.B. Grochow, R.C. Donehower, E.K. Rowinsky, Absorption, metabolism, and excretion of 14C-temozolomide following oral administration to patients with advanced cancer, Clin. Cancer Res. 5 (1999) 309-317.

[11] C.D. Britten, E.K. Rowinsky, S.D. Baker, S.S. Agarwala, J.R. Eckardt, R. Barrington, S.G. Diab, L.A. Hammond, T. Johnson, M. Villalona-Calero, U. Fraass, P. Statkevich, D.D. Von Hoff, S.G. Eckhardt, A Phase I and pharmacokinetic study of temozolomide and cisplatin in patients with advanced solid malignancies, Clin. Cancer Res. 5 (1999) 1629-1637.

[12] D.M. Park, D.D. Shah, M.J. Egorin, J.H. Beumer, Disposition of temozolomide in a patient with glioblastoma multiform after gastric bypass surgery, J. Neuro-Oncol. 93 (2009) 279-283.

[13] K. Hong, P. Likhari, D. Parker, P. Statkevich, A. Marco, C.-C. Lin, A.A. Nomeir, High-performance liquid chromatographic analysis and stability of anti-tumor agent temozolomide in human plasma, J. Pharm. Biomed. Anal. 24 (2001) 461-468.

[14] M. Andrasi, R. Bustos, A. Gaspar, F.A. Gomez, A. Klekner, Analysis and stability study of temozolomide using capillary electrophoresis, J. Chromatogr. B 878 (2010) 1801-1808.

[15] H.K. Kim, C.-C. Lin, D. Parker, J. Veals, J. Lim, P. Likhari, P. Statkevich, A. Marco, A.A. Nomeir, High-performance liquid chromatographic determination and stability of 5-(3-methyltriazen-1-yl)-imidazo-4-carboximide, the biologically active product of the antitumor agent temozolomide, in human plasma, J. Chromatogr. B 703 (1997) 225-233.

[16] M. Andrási, B. Törzsök, A. Klekner, A. Gáspár, Determination of temozolomide in serum and brain tumor with micellar electrokinetic capillary chromatography, J. Chromatogr. B 879 (2011) 2229-2233.

[17] F. Shen, L.A. Decosterd, M. Gander, S. Leyvraz, J. Biollax, F. Lejeune, Determination of temozolomide in human plasma and urine by high-performance liquid chromatography after solid-phase extraction, J. Chromatogr. B Biomed. Appl. 667 (1995) 291-300.

[18] S.K. Chowdhury, D. Laudicina, N. Blumenkrantz, M. Wirth, K.B. Alton, An LC/MS/MS method for the quantitation of MTIC (5-(3-N-methyltriazen-1-yl)-imidazole-4-carboxamide), a bioconversion product of temozolomide, in rat and dog plasma, J. Pharm. Biomed. Anal. 19 (1999) 659-668.

[19] M. Ghalkhani, I.P.G. Fernandes, S.C.B. Oliveira, S. Shahrokhian, A.M. Oliveira-Brett, Electrochemical redox behaviour of temozolomide using a glassy carbon electrode, Electroanalysis 22 (2010) 2633-2640.

[20] P.V.F. Santos, I.C. Lopes, V.C. Diculescu, M.C.U. de Araújo, A.M. Oliveira-Brett, Redox mechanisms of nodularin and chemically degraded nodularin, Electroanalysis 23 (2011) 2310-2319.

[21] I.C. Lopes, P.V.F. Santos, V.C. Diculescu, F.M.P. Peixoto, M.C.U. Araújo, A.A. Tanaka, A.M. Oliveira-Brett, Microcystin-LR and chemically degraded microcystin-LR electrochemical oxidation, Analyst 137 (2012) 1904-1912.

[22] I.C. Lopes, P.V.F. Santos, V.C. Diculescu, M.C.U. de Araújo, A.M. Oliveira-Brett, Sorbic acid and its degradation products: electrochemical characterization, Anal Lett 45 (2012) 408-417.

[23] I.B. Santarino, S.C.B. Oliveira, A.M. Oliveira-Brett, Protein reducing agents dithiothreitol and tris(2-carboxyethyl)phosphine anodic oxidation, Electrochem Commun 23 (2012) 114-117.

[24] E.S. Newlands, M.F.G. Stevenst, S.R. Wedge, R.T. Wheelhouse, C. Brock, Temozolomide: a review of its discovery, chemical properties, pre-clinical development and clinical trials, Cancer Treat Rev 23 (1997) 35-61.

[25] C.M.A. Brett, A.M. Oliveira-Brett, Electrochemistry: Principles, Methods and Aplications, Oxford University Press, Oxford, 1993.

[26] http://www.hbcpnetbase.com/, Handbook of Chemistry and Physics.

[27] E.T. Smith, Examination of n=2 reaction mechanisms that reproduce pH-dependent reduction potentials, Anal. Chim. Acta 572 (2006) 259-264.
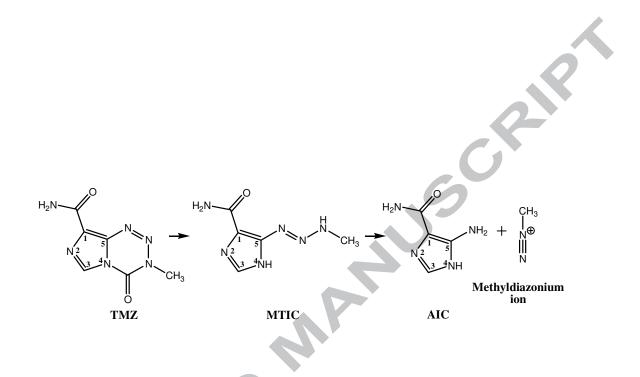
[28] J.R.B. Rodriguez, A.C. Garcia, A.J.M. Ordieres, P.T. Blanco, Electrochemical oxidation of dacarbazine and its major metabolite (AIC) on carbon electrodes Electroanalysis 1 (1989) 529-534.

Figures

Scheme 1. Hydrolysis cascade of TMZ to MTIC and their metabolites, AIC and methyldiazonium ion, in aqueous solution.
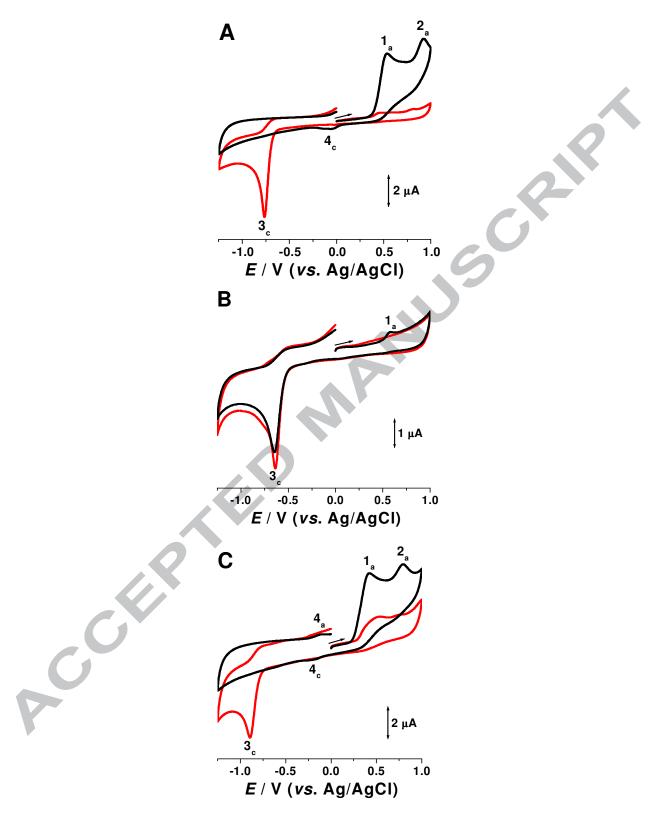
Fig. 1. CVs in 600 µM TMZ (—) freshly prepared solution and (—) after 7 days incubation in: **(A)** 0.1 M phosphate buffer pH = 7.0; **(B)** 0.1 M acetate buffer pH = 4.1 and **(C)** 0.1 M borax buffer pH = 9.2, saturated with N_2, $v = 100$ mV s^{-1}.

Fig. 2. DP voltammograms in 250 µM TMZ: (—) freshly prepared solution and after (•••••) 1 h, (---) 1 day and (—) 7 days incubation, $v = 5$ mV s^{-1}.

Fig. 3. UV-Vis absorption spectra of 50 µM TMZ (—) freshly prepared solution and after (•••••) 30 min, (•••) 2 h (---) 2 days and (—) 7 days incubation in: **(A)** 0.1 M phosphate buffer pH = 7.0; **(B)** 0.1 M acetate buffer pH = 4.1 and **(C)** 0.1 M borax buffer pH = 9.2.

Fig. 4. Successive CVs in 250 µM cdTMZ in 0.1 M phosphate buffer pH = 7.0: (—) first, (---) second and (•••••) third scans, $v = 100$ mV s^{-1}.

Fig. 5. (**A**) DP voltammograms in 250 µM cdTMZ as a function of pH. (**B**) Plot of E_p of peaks (■) 1_a and (●) 2_a and I_p of peaks (□) 1_a and (○) 2_a vs. pH.

Fig. 6. DP voltammograms in 250 µM cdTMZ in 0.1 M phosphate buffer pH = 7.0: (━)
first and (━) second scans between + 0.1 V e + 0.6 V and (━) first and (━)
second scans between + 0.1 V e + 1.0 V.

Fig. 7. SW voltammograms in 250 µM cdTMZ in 0.1 M phosphate buffer pH = 7.0: (**A**)
first and (**B**) second scans; I_t – total current, I_f – forward current and I_b –
backward current, v_{ef} = 100 mV s^{-1}.

Scheme 1. Hydrolysis cascade of TMZ to MTIC and their metabolites, AIC and

methyldiazonium ion, in aqueous solution.

Fig. 1. CVs in 600 µM TMZ (━) freshly prepared solution and (━) after 7 days incubation in: **(A)** 0.1 M phosphate buffer pH = 7.0; **(B)** 0.1 M acetate buffer pH = 4.1

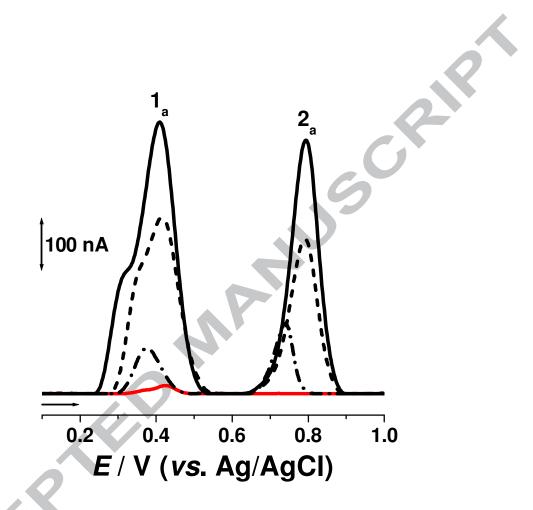and (**C**) 0.1 M borax buffer pH = 9.2, saturated with N_2, $v = 100$ mV s^{-1}.

Fig. 2. DP voltammograms in 250 μM TMZ: (━) freshly prepared solution and after
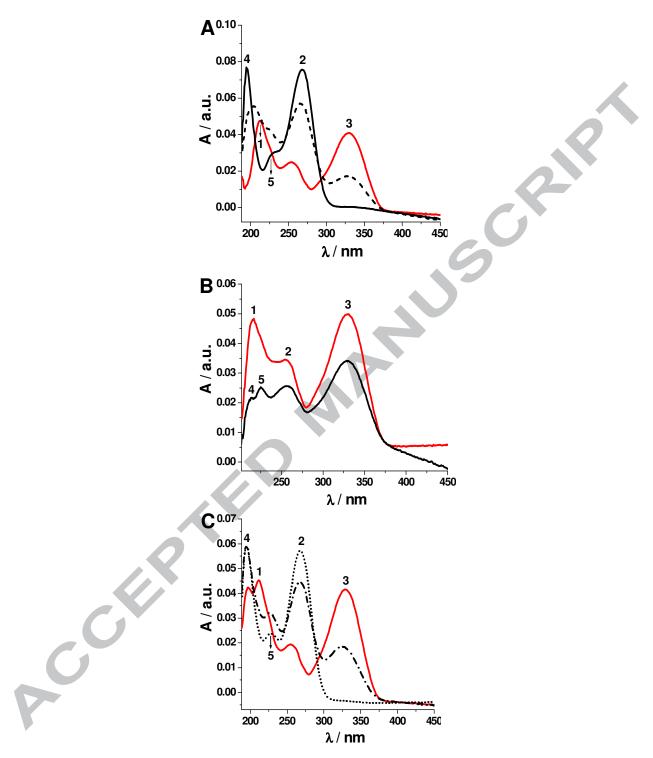(•••••) 1 h, (---) 1 day and (━) 7 days incubation, v = 5 mV s^{-1}.

Fig. 3. UV-Vis absorption spectra of 50 µM TMZ (▬) freshly prepared solution and after (•▬•▬•) 30 min, (•••) 2 h (▬▬▬) 2 days and (▬) 7 days incubation in: **(A)** 0.1 M phosphate buffer pH = 7.0; **(B)** 0.1 M acetate buffer pH = 4.1 and **(C)** 0.1 M borax buffer pH = 9.2.
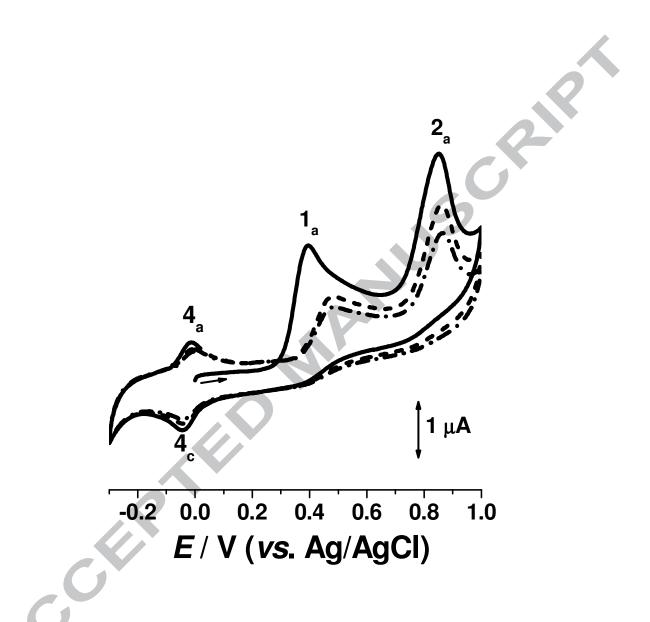
Fig. 4. Successive CVs in 250 μM cdTMZ in 0.1 M phosphate buffer pH = 7.0: (—) first, (---) second and (•••••) third scans, v = 100 mV s^{-1}.

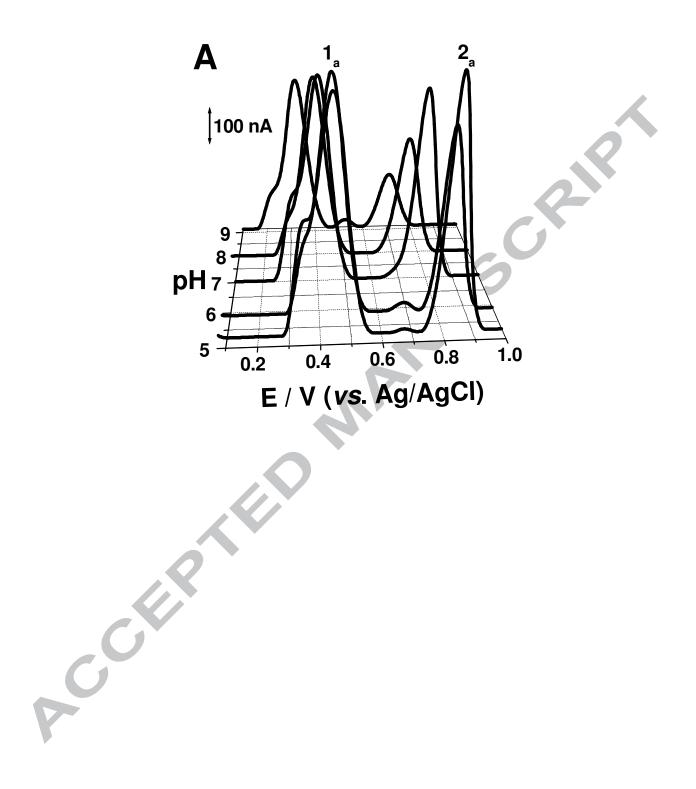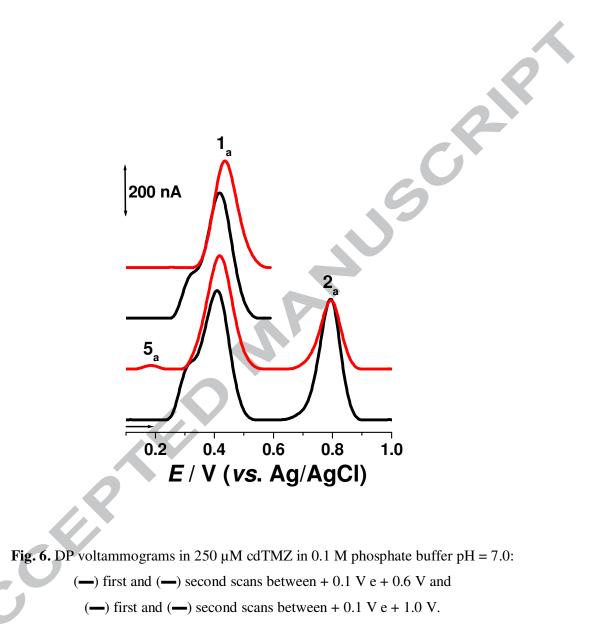**Fig. 5.** (**A**) DP voltammograms in 250 µM cdTMZ as a function of pH.

(**B**) Plot of E_p of peaks (■) 1_a and (●) 2_a and I_p of peaks (□) 1_a and (O) 2_a *vs*. pH.

Fig. 6. DP voltammograms in 250 μM cdTMZ in 0.1 M phosphate buffer pH = 7.0:
(—) first and (—) second scans between + 0.1 V e + 0.6 V and
(—) first and (—) second scans between + 0.1 V e + 1.0 V.
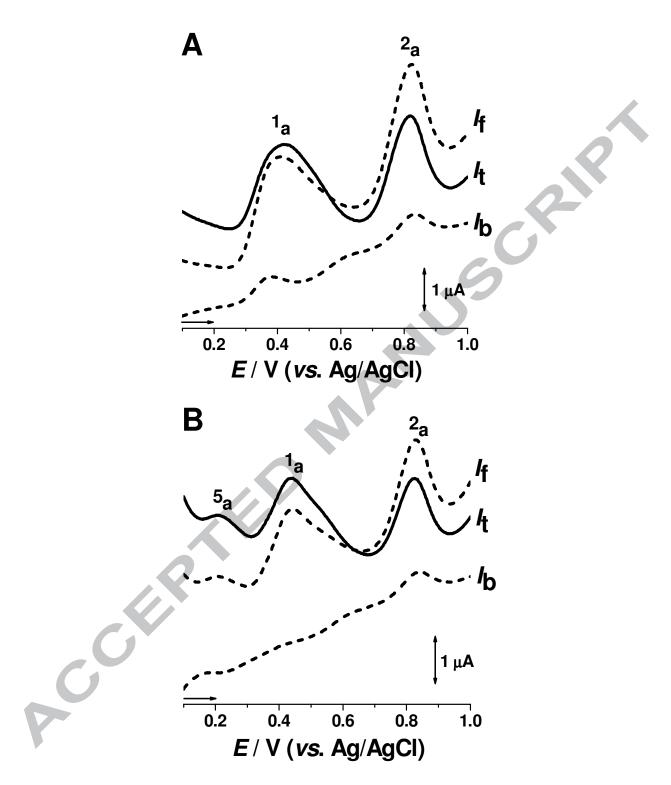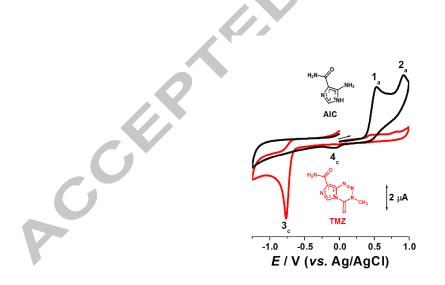
Fig. 7. SW voltammograms in 250 μM cdTMZ in 0.1 M phosphate buffer pH = 7.0: (**A**) first and (**B**) second scans; I_t – total current, I_f – forward current and I_b – backward current, $v_{ef} = 100$ mV s^{-1}.

Temozolomide chemical degradation to 5-aminoimidazole-4-carboxamide – Electrochemical study

Ilanna C. Lopes, Severino Carlos B. de Oliveira, Ana Maria Oliveira-Brett[*]

Departamento de Química, Faculdade de Ciências e Tecnologia, Universidade de

Coimbra, 3004-535 Coimbra, Portugal

Graphical Abstract

CVs in 600 µM TMZ in 0.1 M phosphate buffer pH = 7.0, saturated with N_2: (—) freshly prepared solution and (—) after 7 days incubation, v = 100 mV s^{-1}.

Temozolomide chemical degradation to 5-aminoimidazole-4-carboxamide – Electrochemical study

Ilanna C. Lopes, Severino Carlos B. de Oliveira, Ana Maria Oliveira-Brett[*]

Departamento de Química, Faculdade de Ciências e Tecnologia, Universidade de

Coimbra, 3004-535 Coimbra, Portugal

Highlights

- The chemical degradation of temozolomide was investigated electrochemically.

- Temozolomide undergoes degradation to 5-aminoimidazole-4-carboxamide (AIC).

- The electrochemistry oxidation of AIC at a glassy carbon electrode was studied.